Residential Building Site Suitability Assessment and Mapping, Philippines

Olaf Neussner[1]

[1]Independent consultant - olafneus@gmail.com

Keywords: Site Suitability Assessment, Average Annual Loss, Natural Hazards, Probabilistic Risk Assessment

Abstract

This paper suggests a novel method to site suitability mapping in the Philippines. In a country where natural hazards pose a serious threat to human development the assessment of the potential impacts of such hazards is of central importance. However, up to now, no comprehensive, nationwide, probabilistic risk assessments have been conducted resulting in vague qualitative risks estimations and in turn large uncertainties for site suitability assessments. Taking asset-specific vulnerabilities into consideration, the new approach here estimates the physical damage caused by six natural hazards, and this leads to a solid risk estimation with a resolution of 30 m. Such an estimation forms the backbone of site suitability. Other factors influencing suitability depend largely on subjective preferences like the closeness of hospitals or shopping facilities. The suggested method can facilitate an infinite number of factors if they can be geographically located. As an example, the proximity to population and to roads was introduced here. A single, detached, residential building with medium fragility served as a sample asset. The risk assessment revealed a strong gradient of risk, and by extension site suitability, from relatively low values for the southwest to higher values in the north of the Philippines, if all other factors are equal. Coastal areas are especially at risk because of the tsunami and storm surge hazards and thus, generally less suitable for residential buildings.

1. Introduction

Site suitability mapping with Geographical Information Systems (GIS) is a well-established method of identifying locations appropriate for specific assets. The technique widely used in a GIS application is the multicriteria decision analysis (Malczewski, 2004). Suitability models might aid in finding a favorable location for a new facility, road, building or crops. In the Philippines suitability assessments focused mainly on agricultural production, specifically crops in the past (Bato, V. A., 2018; Department of Agriculture, Western Visayas, no date; Francisco et al., 2024; Garcia, 2021; Gavino, 2020; PCA, 2023; BSWM, 2025) and in one case on a landfill (Sadie, 2022). Land use planners, potential homeowners, and insurance companies are interested in location suitability of residential houses. However, studies to determine risks and convenience of locations for housing development in the Philippines are few (Sia, 2021; Morales, 2021; GIZ, 2015) although the official guidelines prescribe suitability analysis as a step in the development of mandatory Comprehensive Land Use Plans, CLUP (HLURB, 2013). It is suspected that the shortage of methods of site suitability mapping results in relatively few studies utilizing assessment tools for urban or settlement planning purposes. This paper aims to contribute to methodological improvements and user-friendly approaches of visualizing results of suitability assessments. It is drawing from experiences in other countries (Al-Shalabi, 2006; Purwaamijaya, 2020; Lin, 2015; Murseli, 2014; Luan, 2021; Huang, 2019).

According to the Philippine Statistics Authority, single, residential houses were the most common building type in the Philippines in 2020 with a total number of 22 million occupied housing units. This represents 87.6 percent of all housing units (PSA, 2023). It is believed that most of the single houses were built without proper assessment of suitability and risk considerations. Based on data from PSA, 2.8 mil. houses suffered either damage or total destruction in the nine-year period from 2015 to 2023 (PSA, 2025). This is equivalent to an annual hit rate of 2.8% of all residential houses and an unacceptable high number. 96% of housing damage was caused by tropical cyclones, 3% by earthquakes and the remaining 1% by a spectrum of other hazards (PSA, 2025). The picture looks similar in economic terms. 86% of damage (USD) originates from storms, 11% from floods, and 1% from earthquakes (CRED, 2025).

The suitability of a location is strongly influenced by the expected impact of natural hazard events. Naturally, a low impact is preferred, and the assessment of possible impacts plays a major role in the estimation of damage and loss. This may be facilitated by a worst-case scenario, but this approach does not reveal how likely such scenario is and the method giving more realistic information is a probabilistic assessment with different return periods or probabilities. This requires probabilistic hazard data. Although official Philippine guidelines do not explicitly prescribe to use data from Philippine governmental institutions, most official users turn to such data first before considering others.

Three institutions of the Philippine government are tasked with producing information, including maps, of natural hazards. The Philippine Atmospheric, Geophysical and Astronomical Service Administration (PAGASA) is responsible for meteorological, climatic, and storm surge hazards. The Philippine Institute for Volcanology and Seismology (PHIVOLCS) takes care of volcano, earthquake, tsunami, and earthquake-induced landslide hazards, while the Mines and Geosciences Bureau (MGB) produces flood and rain-induced landslide hazard information. Most of the published hazard maps are qualitative maps showing hazards in categories of low, medium, and high hazard or are susceptibility maps indicating that the occurrence of a hazard is physically possible without providing any information on the likelihood or intensity/severity of a possible hazard event. This leaves the suitability assessment with a gap that must be filled to arrive at a useful estimation of expected damage with a reference period of one year. Apart from Philippine government offices, there are other institutions in the country and abroad producing various hazard maps. Some of those are probabilistic but may be on global scale with a lower resolution than some locally produced maps.

Estimations of expected damage are dependent on the vulnerability of an asset with regards to the forces of an extreme hazard event. Thus, data on the fragility of specific assets are required for the calculation of expected damage. Single, residential houses are a common asset in the Philippines, but not many vulnerability data are available. Such data originates from historical observations or from models. Some surveys were conducted after disasters resulting in large numbers of affected houses, but they focused on other aspects than developing vulnerability curves (Mas, 2014; Graciano 2020) or the vulnerability curves covered other types of buildings (Baylon, 2022, Acosta, 2018, 2022). One publication reported the results of expert opinion on the fragility of non-engineered residential buildings in Batanes, Philippines, for tropical cyclones and earthquakes (Hadlos, 2023). The gaps in locally available fragility functions were filled with data from other countries with comparable housing structures.

Probabilistic hazard maps and vulnerability data are sufficient to determine expected annual losses for different hazard probabilities, and these losses may be combined to arrive at a total Average Annual Loss (AAL) expressed as the percentage of loss of the value of an asset. Losses from different hazards add up to a multi-hazard AAL (Figure 1) under the assumption that hazard events do not depend on each other and that the time between events enables repairs to establish the original value of an asset.

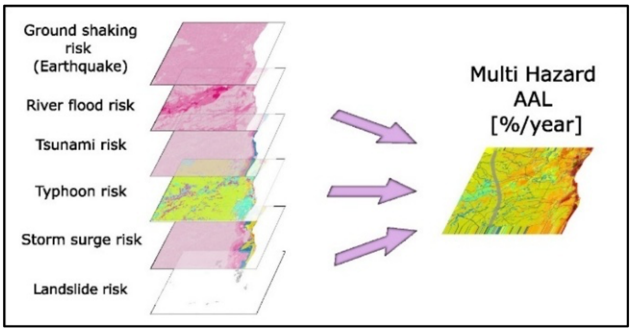

Figure 1. Composition of the multi-hazard Average Annual Loss (AAL) in percentage of asset value.

The suitability of a site for a specific type of land use is not only determined by the danger posed by natural hazards but also by a potentially infinite number of other criteria. These criteria may be socio-economic or environmental, or any other aspect deemed important. While the assessment of expected damage caused by extreme events may be calculated using solely physical characteristics and calculated frequencies and severities of natural hazards, the other site suitability criteria are personal or community preferences and may be determined on a case-to-case basis. For example, the suitability of the location of a shop may call for a high density of population near the place while a factory handling dangerous chemicals may use this criterion in the opposite way to expose few people to hazardous substances in case of an accident. There is no way of directly comparing the danger emanating from natural hazards with community-defined socio-economic or other criteria. The way around this incompatibility is the introduction of indices (Malczewski, 2004). Using indices involves developing an optimization derived from heterogeneous data. This is a challenge because weights given to parameters depend on subjectivity (Malczewski, 2004). The approach chosen here relies on quantitative suitability criteria only, such as the maximum acceptable AAL or proximity to a road. This avoids the subjective character of index boundaries.

2. Materials and Methods

The site suitability map is based on six hazards (ground shaking, landslides, river floods (incomplete), tsunamis, storm surges, and windstorms), and the proximity to population and roads with a horizontal resolution of 30 m.

2.1 Data Sources

The datasets are open data retrieved from public geospatial data sources with a preference for more recent and higher horizontal resolution data when more than one source was available.

Topographic data was solicited from Forest And Buildings removed Copernicus Digital Elevation Model, FABDEM (Uhe, 2022) with a horizontal resolution of ~30m. This DEM is relatively new, and it utilizes a wider spectrum of earth observation sources compared to older models, thus reducing inaccuracies. Population density with a resolution of 100m and data of 2020 came from the Joint Research Center (JRC) of the European Commission (Carioli, 2023). Land cover with a resolution of 30m as of 2022 was provided by the Philippine Space Agency, PhilSA, as the newest land cover map made in the Philippines with a local set of classes. Blanks in that dataset were filled with data from the European Space Agency (ESA, 2021, 10m resolution). Administrative borders came from the National Mapping and Resource Information Authority of the Philippines (NAMRIA) via Humanitarian Data Exchange (HDX, 2023). The proximity to roads was calculated based on vector data from Open Street Map (OSM, no date). Probabilistic river flood hazard data is either incomplete or at a low resolution. Data was utilized from Project NOAH (National Operational Assessment of Hazards) of the Resilience Institute of the University of the Philippines, UPRI (no date, identical with data of the Disaster Risk and Exposure Assessment for Mitigation (DREAM) program of the UP). A gap in the data was filled with data from the Joint Research Center (JRC, 2024), but still large areas of the country are not included in the used datasets. The direction of storms was characterized by data from the International Best Track Archive for Climate Stewardship, IBTrACS (NOAA, 2025). Probabilistic regional wind speeds were acquired from United Nations Office for Disaster Risk Reduction with a resolution of 30km (UNDRR, 2015). They are comparable to data from PAGASA (Cinco, 2013), but these are not available in GIS-ready formats. The wind shielding and roughness factors were taken from Geoscience Australia (Yang, 2014). The National Hurricane Center published an estimation of the correlation between wind speeds and storm surge heights (NHC, no date). That data was combined with storm surge maps published by University of the Philippines (UPRI, no date), and regional wind speed maps (UNDRR, 2015). Ground shaking (earthquake) data with Peak Ground Acceleration (cm/s^2) for 0.2s frequency were used (CAPRA, 2017). That frequency is typical for damage to small buildings. Tsunamis were characterized with data from the Global Tsunami Model (GTM, no date). Data was accessible online before, but the data source is currently (Aug. 2025) offline (geonode-gfdrrlab.org). Historical landslides were taken from the catalogues of the University of Sheffield (Froude, 2018), the National Aeronautics and Space Administration (NASA, no date), a landslide susceptibility raster file of University of the Philippines (UPRI,

https://doi.org/10.5194/isprs-archives-XLVIII-5-W4-2025-175-2026 |

no date), and point data from the University of the Philippines, School of Environmental Science and Management (SESAM, no date). An "average" Philippine single, detached, residential building with semi-concrete steel posts, or with reinforced concrete posts, and with lightweight roofing (Hadlos, 2023) was chosen an example of an asset. It is comparable to the "concrete" category of PAGASA (Monteverde, 2014). The fragility of the described buildings was characterized with data for wind and flood (GIZ, 2014), tsunami and storm surge (Suppasri, 2012), and earthquake (Global Earthquake Model Foundation, no date).

2.2 Data Processing and Analysis

All calculations were performed in WGS84 (EPSG 4326) with QGIS (Version 3.40.6), except for the System for Automated Geoscience Analysis (SAGA, Version 9.4.1) for the Wind Exposure Index (WEI). Calculations were performed in two steps. The first is the production of probabilistic hazard data, and the second is the conversion to damages (Average Annual Loss, AAL).
The AAL is the sum of losses weighted by their probabilities (Equation 1).

$$AAL = \sum_{i=1}^{n} (P_i \; x \; L_i) \quad (1)$$

Where: AAL = Average Annual Loss
P = Probability
L = Loss

The calculated AALs of the six hazards are added under the assumption that each hazard event consists of only one hazard and that the time between extreme events is sufficient to repair damages. This is a simplification as some hazards are interconnected (e.g., floods caused by heavy rain of a typhoon). However, it is unlikely that the integration cascading hazards effects would change the picture substantially. The calculation of return periods and intensities/severities for the six hazards is explained below. For each hazard the combined AAL was calculated as explained above.

2.2.1 Tropical cyclones: The calculation of local wind speeds was performed with three multipliers of regional wind speeds. These are adjustments for the prevailing wind direction, topography, and surface roughness (Figure 2).

Regional wind speeds were converted into local wind speeds by upsampling the regional wind speeds to a resolution of 30m (QGIS, raster converted to points, TIN interpolation). The typical track directions of tropical cyclones shift from the south to the north (Figure 3), and the direction multiplier M_d was accordingly estimated for the south, center, and north of the Philippines (Figure 4).

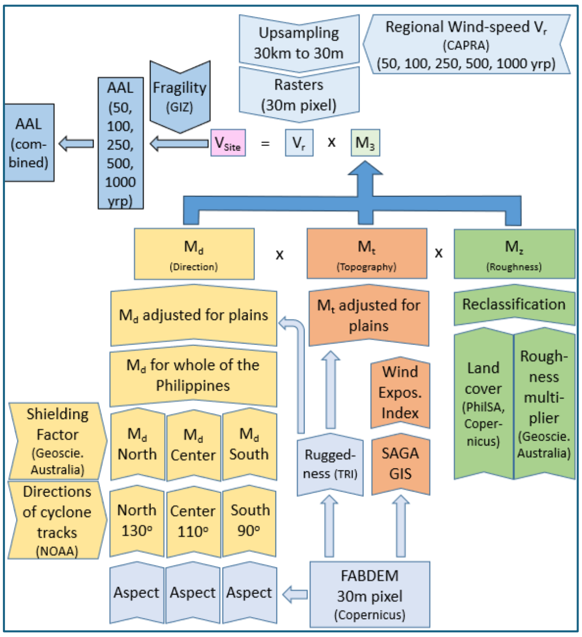

Figure 2. Technical flow to calculate local wind speeds and Average Annual Losses.

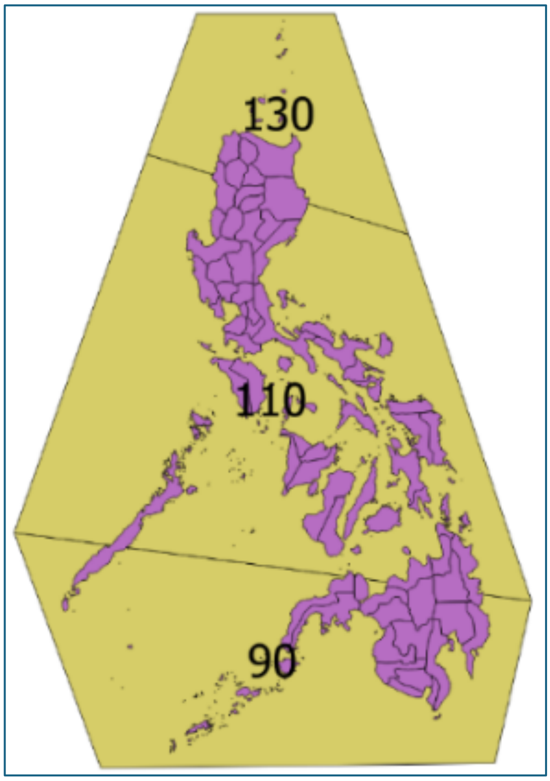

Figure 3. Main wind direction zones with indication of prevailing storm direction in degrees

The aspect was calculated with the FABDEM and factors from Geoscience Australia. Small changes in altitude in the DEM in plain areas resulted in aspect changes resulting in relatively large changes in wind speed. This appears to be unrealistic for plains and the influence of the aspect on the wind speed was reduced with a correction factor derived from ruggedness (QGIS, Terrain Ruggedness Index, TRI).

https://doi.org/10.5194/isprs-archives-XLVIII-5-W4-2025-175-2026 | © Author(s) 2026. CC BY 4.0 License.

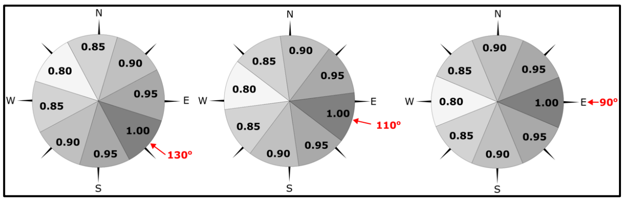

Figure 4. M_d values for three wind direction zones

The topographic multiplier M_t was derived from the Wind Exposure Index (WEI) calculated in SAGA with default settings. The result was noisy for plains, and it was corrected using the TRI.
The roughness multiplier M_r is based on land cover maps (PhilSA, ESA) and factors from Geoscience Australia (GA). For each PhilSA/ESA land cover class, a corresponding class in the GA classification was selected and the respective multiplier applied.

2.2.2 Storm surges: NOAH published storm surge inundation maps with Storm Surge Advisory (SSA) levels numbered 1 to 4 indicating increasing storm surge severities. Each level is divided into three flood intensities (low, medium, high). This results in 12 classes (Table 1).

SSA number (NOAH)	Flood intensity (NOAH)	WS (km/h)	Water height (m)
1	Low	>144 - 157	>1.5 >=2.0
	Medium	>157 – 171	>2.0 >=2.5
	High	>171 – 184	>2.5 >=3.0
2	Low	>184 – 193	>3.0 >=3.3
	Medium	>193 – 202	>3.3 >=3.7
	High	>202 – 210	>3.7 >=4.0
3	Low	>210 – 218	>4.0 >=4.3
	Medium	>218 – 229	>4.3 >=4.7
	High	>229 – 237	>4.7 >=5.0
4	Low	>237 – 250	>5.0 >=5.5
	Medium	>250 – 263	>5.5 >=6.0
	High	>263	>6.0

Table 1. NOAH levels and corresponding water heights above tide level (SSA: Storm Surge Advisory level).

The water height at the seashore was determined by using regional wind speeds (see above) and a correlation between wind speeds and water heights published by NOAA. This is an approximation and local bathymetry, and other factors may cause considerable different water heights. A combination of the NOAH and the NOAA data was used to estimate storm surge water heights. This was determined by assuming a linear dependency [y = (x - 104.12)/26.559]. This is a simplification as the real correlation is slightly non-linear. The fragility of single, residential buildings is assumed to be like tsunami vulnerability (see below), and calculations of AAL were performed accordingly in the same manner as the AAL for tropical cyclones.

2.2.3 Tsunami: The data is TIF files with selected points for the Philippines for 10, 50, 100, 500, 1000, and 2500 years return periods. The gaps between the points were filled in QGIS by buffering around the points. The area susceptible to inundation depending on the water height at the coastline was calculated by deducting the FABDEM height from the buffer values.

The author is not aware of local tsunami building fragility data for the Philippines, but the fragility of buildings in Japan after the tsunami in 2011 is very well documented for many different building types (Suppasri, 2013). One similar to the Philippines was selected for damage calculations (Table 2).

Inundation depth [m]	Damage cost in % of value
0.1 - 0.5	32.0
>0.5-1.0	49.7
>1.0-1.5	62.1
>1.5-2.0	75.0
>2.0-2.5	85.6
>2.5-3.0	92.0
>3.0-3.5	95.5
>3.5-4.0	97.1
>4.0-4.5	97.6
>4.5-5.0	97.9
>5.0-5.5	98.6
>5.5-6.0	98.9
>6.0-6.5	99.0
>6.5-7.0	99.2
>7.0-7.5	99.2
>7.5-8.0	99.1

Table 2. Tsunami water height and corresponding damage.

2.2.4 Landslide: Data from NOAH indicating landslide susceptibility is the basis for estimating the probabilities for landslides. The size of the landslide-prone area was determined to be 135,000 km^2 or 45% of the land area of the country. The probability of landslides in the three categories of NOAH (low, medium, high) was estimated by taking documented landslides (see data sources) over a period of about ten years and calculating their annual frequency for each class. The number of documented landslides appears to be very low. An educated guess suggests a number 20 times higher. This estimated value was used for further calculations.

The average size of landslides was estimated with a visual survey of landslide scars visible on Sentinel 2 images. An upper value (0.01 km^2) was selected for further processing. The probabilities were used to calculate the AAL with the assumption that a residential building hit by a landslide will be destroyed completely (Table 3).

	NOAH Category		
	1	2	3
Number of landslide records (~10 years)	70	264	361
Estimated number of landslides (records x 20)	1,400	5,280	7,220
Estimated landslide area (km^2)/10 years	1.4	5.3	7.2
Estimated landslide area (km^2)/year	0.14	0.53	0.72
Hazard area according to NOAH (km^2)	17,341	56,619	61,040

Number of years until all of hazard areas are subjected to landslides	124k	107k	85k
Landslide probability	0.000008	0.000009	0.000012

Table 3. Calculation of landslide probability based on records and estimations.

2.2.5 River flood: Project NOAH and the DREAM project published flood hazard maps for three different return periods, 5, 25, and 100 years (Table 4). Color coded categories correspond to inundation heights.

Category	5 yrp (m)	25 yrp (m)	100 yrp (m)
1	0.1	0.5	0.5
2	0.3	0.75	1.0
3	0.5	1.0	1.5

Table 4. Flood water heights by category and return period (yrp).

Unfortunately, the NOAH/DREAM data does not cover the whole country. Large parts of the Agusan River basin are missing in the NOAH/DREAM data, but some 100yrp data are available from JRC and they were combined with the NOAH data. Vulnerability data (GIZ, 2015) was used for AAL calculations.

2.2.6 Earthquake: Most of the ground shaking hazard maps available are either not probabilistic or not available in GIS-ready formats. The source (CAPRA, 2017) used for the site suitability assessment is available in GIS-ready formats, but it may not be the one reflecting reality best. Data appropriate for single residential houses have a frequency of 0.2 s and CAPRA provides Peak Ground Acceleration for 250, 475, 975, 1475, and 2500 years return period. Vulnerability data came from the Global Quake Model for a building type comparable to the Philippine setting (unreinforced concrete block masonry, lime/cement mortar, reinforced concrete floors/roof).

2.2.7 Population proximity: In the context of the Philippines, 1 km may be regarded as walking distance; therefore, a circle with a radius of 1 km was chosen as a sample factor influencing the suitability of a location.

The JRC's population density reflects how many people reside in a hectare (100 m x 100 m). The pixels of the JRC map (TIF) were converted to vector points (QGIS: Raster Pixels to Points) and a buffer of 1 km radius was created for each point. For each buffer the sum of the values for the population density raster file was calculated (QGIS: Raster Analysis – Zonal Statistics: Sum). Each circular buffer is converted to a vector point with the attribute *sum* (QGIS: Centroids).

2.2.8 Road proximity: The OSM shapefile containing roads formed the basis for estimating distances to the next road from all points of the site suitability map. All objects not accessible by a four wheeled vehicle were neglected (stairs, footpath, etc.) and the remaining roads (vector lines) were converted to points. QGIS provides an algorithm for calculating the distance to the next point (Distance to Nearest Hub (Points)) and this resulted in a new attribute with the respective distance for all map points. The AAL values for the six hazards and the values for population and road proximity were combined in the attributes of a point vector file. For raster files, the value of the raster file was extracted with the Point Sampling Tool of QGIS (Plugin).

3. Results

The overview map of multi hazard AALs exhibits a clear gradient from the south-west to the north (Figure 5). The latter is subject to much more damage than the south-west. The main reason for this phenomenon is the occurrence of tropical cyclones. The typical path of typhoons is from the central east to the northwest leaving the southwest largely untouched.

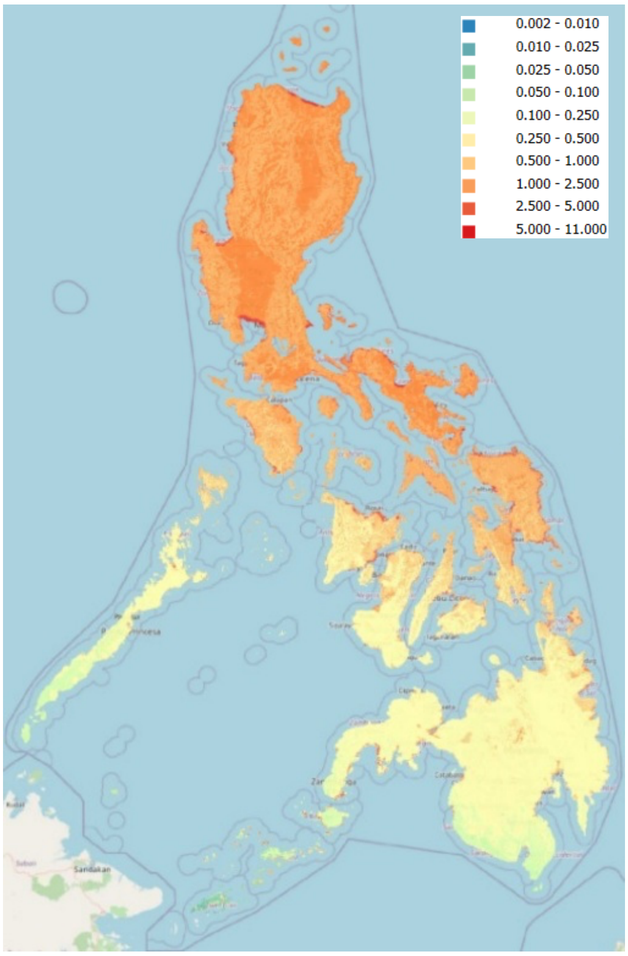

Figure 5. Average Annual Loss in percentage of asset value.

On the local level, the strong influence of storms on the multi-hazard AAL is striking. In Figure 6 the eastern slopes of mountains exhibit much higher AAL values than the western slopes. The reason for this pattern is the dominant direction of tropical cyclones the Philippines. Their trajectory is predominantly westward, with a minor northward vector.

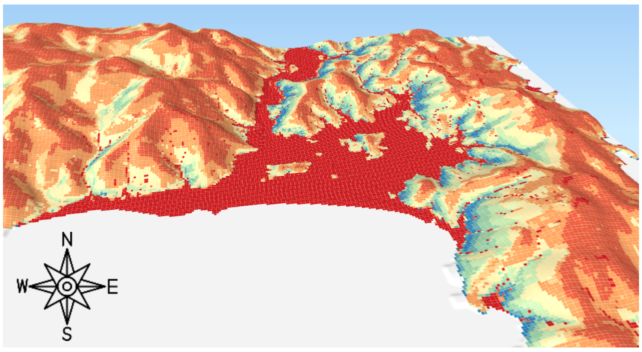

Figure 6. Example of a 3-D view of the south eastern part of the island of Catanduanes. Legend is the same as in Fig. 5.

The site suitability map has a resolution of about 30 m, and it exhibits strong local differences in expected AAL as many hazards are limited to a specific area (e.g. floods), while hazards like storms and earthquakes have fuzzy borders. Low lying, coastal areas are most at risk from extreme natural hazard events as storm surges and tsunamis add to fuzzy hazards.

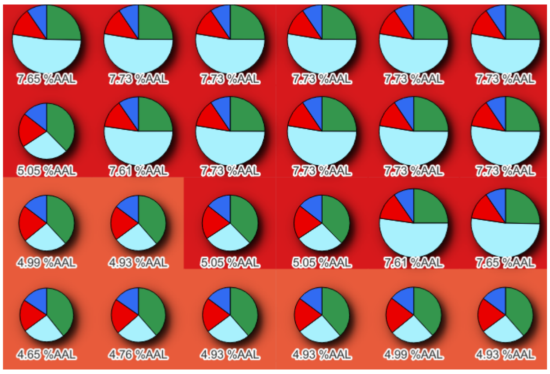

Figure 7. Sample map with total AAL (numbers) and contribution from hazards (pie slices, dark blue: river flood, light blue: tsunami, green: storm surge, red: storm). The distance between the centers of the circles is 30 m. The background color and the size of the pie signify the magnitude of the AAL.

The composition of the AALs and the total AALs can be displayed as a pie chart for each point in QGIS (Figure 7). The vector point data enables a user to filter with a set of criteria for areas matching certain conditions. In QGIS features may be selected with the Select Features interface (Figure 8).

The data are available on request from the author.

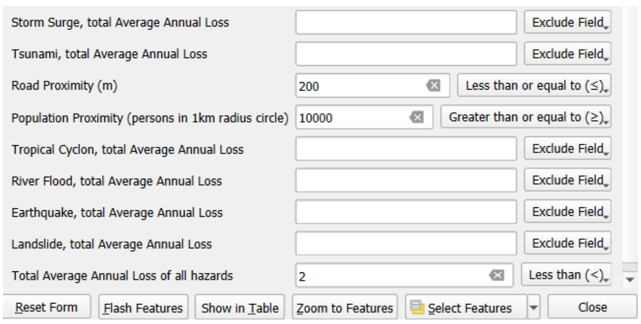

Figure 8. Example of filtering with the conditions of roads closer or equal to 200 m away, at least 10,000 persons within a 1 km radius and less than a total 2% AAL.

Figure 8. Example of filtering with the conditions of roads closer or equal to 200 m away, at least 10,000 persons within a 1 km radius and less than a total 2% AAL.

4. Conclusions

The residential building site suitability map introduces a novel way of quantifying and visualizing risk in connection with other factors in the Philippines. Probabilistic hazard analysis enables a quantitative way of describing risk in monetary terms, which is more tangible than an index. The proposed GIS-based map enables a user to integrate any other factors deemed to be of relevance to the selection of a site. Such factors are mostly distances to services like health, education, public transport or population proximity. The latter is important for businesses looking for locations with many potential customers within walking or motorized distances. Land-use planners may use the site suitability map for the identification of new settlement sites or safe locations for essential services like a Disaster Risk Reduction and Management office, a hospital, or a power plant (the respective vulnerabilities are needed for that application). Catastrophe insurance companies may not be very interested in the “other factors” but just in the risk of a home. The suggested method is flexible in terms of hazards and other factors. Other hazards may be added if reliable, probabilistic data are available. Many GIS-compatible datasets are available (e.g., location of hospitals) and may be treated like the distance to the next road resulting in the distance to the hospital.

It is difficult to verify the results of risk assessments (including site suitability) as the ultimate proof is the occurrence of extreme events and resulting damage. For relative frequent hazards like cyclones and river floods such events are frequent enough to warrant some statistical analysis of past events while earthquakes and tsunamis are on the level of anecdotal evidence. There are several factors influencing the accuracy of the results. Obviously, the quality of the results cannot be better than the quality of the input data. Though the quality of the data sources is not discussed in detail in this paper, it is noteworthy that different sources describing the same phenomena often exhibit substantially different data. This applies to probabilistic hazard data as well as to fragility curves of buildings, and some other data sources (e.g., land cover maps). A rough check of the reliability of the data was performed and the most trustworthy selected. However, there is certainly room for improvement. This applies, for example, to the river flood hazard. Data is incomplete and does not cover the whole country. Furthermore, only six hazards were used. Though they may be responsible for most damage other hazards may be locally important too (e.g. volcanos). Vulnerabilities are a simplification and if specific vulnerabilities of a particular asset are known the resulting AAL will be more realistic. Future developments of the method should include more hazards, updating or completing included hazards, a web-based interface and a selection of vulnerability data for other assets.

Acknowledgement

The development of the site suitability method started with work of the author for the Deutsche Gesellschaft für Internationale Zusammenarbeit (GIZ) a decade ago. It benefited from experiences of the author with risk mapping supported by the United Nations Office for Disaster Risk Reduction, UNDRR.

References

Acosta, T.J.S., Galisima, J.J., Tana, L.R., Hernandez Jr., J.Y., 2018: Development of Empirical Wind Vulnerability Curves of School Buildings Damaged by the 2016 Typhoon Nina. *Procedia Engineering* 212 (2018) 395–402

Acosta, T.S., 2022: Risk assessment of low-rise educational buildings with wooden roof structures against severe wind loadings. *Journal of Asian Architecture and Building Engineering*, 21:3, 973-985, DOI: 10.1080/13467581.2021.1909596

Al-Shalabi, M.A., Mansor, S.B., Ahmed, N.B., Shiriff, R., 2006: GIS Based Multicriteria Approaches to Housing Site Suitability Assessment, XXIII FIG Congress, fig.net/resources/proceedings/fig_proceedings/fig2006/papers/ts72/ts72_05_alshalabi_etal%20_0702.pdf (15 August 2025)

Bato, V. A., 2018: GIS-based suitability mapping of banana in the Philippines. *ISSAAS* Vol. 24, No. 1: 1-13

Baylon, M.B., Maria Emilia P. Sevilla, M.E.P., Cutora, M.DL., Villa, R.M.S., Reynes, P.M.P., Montemayor, J.M.V., 2022: Development of fragility curves for seismic vulnerability assessment: The case of Philippine General Hospital spine building, *International Research Journal of Science, Technology, Education, and Management*, vol. 2 no. 4

Bureau of Soils and Water Management, BSWM, 2025: BSWM maps (107 maps). bswm.da.gov.ph/bswm-maps/? (16 August 2025)

Central American Probabilistic Risk Assessment, CAPRA, 2017. risk.preventionweb.net/ (20 August 2025)

Carioli, A., Schiavina, M., Freire, S., MacManus, K., 2023: GHS-POP R2023A - GHS population grid multitemporal (1975-2030). European Commission, Joint Research Centre (JRC) [Dataset] doi: 10.2905/2FF68A52-5B5B-4A22-8F40-C41DA8332CFE

Centre for Research on the Epidemiology of Disasters, CRED, 2025: EM-DAT - Country Profiles, Philippines. data.humdata.org/dataset/emdat-country-profiles-phl (16 August 2025)

Cinco, T., 2013: Tropical cyclone severe wind risk modelling in GMMA, Presentation at the 2013 APEC Typhoon Symposium in Taipei

Department of Agriculture, Western Visayas, no date: Suitability map. westernvisayas.da.gov.ph/suitability-map/, (14 August 2025)

Deutsche Gesellschaft für Internationale Zusammenarbeit, GIZ, 2015: Residential Building Suitability Map for Leyte Island, Philippines. preventionweb.net/files/47118_47118 suitabilitymapsfinalversion121.pdf (07 August 2025)

Francisco, J.T., Casisirano, J.D., Blanco, A.C., Rivera, R.L., Canja, L.H., Francisco, M.D., Barrientos, R.M., 2024: Enhancement of the field assessment protocols and suitability maps for coconut. *Int. Arch. Photogramm. Remote Sens. Spatial Inf. Sci.*, XLVIII-4/W8-2023, 251–258

Froude, M.J., Petley, D.N.: Global fatal landslide occurrence from 2004 to 2016, 2018. *Nat. Hazards Earth Syst. Sci.*, 18, 2161–2181, 2018

Garcia, K.R.S., Umali, B.P., Flores, J.A., Videna, B.S., Bagasin, C.C., Herrera, J.L.B., Sedigo, N.a., 2021: Philippine land suitability assessment and mapping for Coffea arabica and Coffea liberica production using Geographic Information System (GIS) and Multi-Criteria Decision Making (MCDM) Techniques. *Philippine Coffee Journal* 2, 1-17

Global Earthquake Model Foundation (GEM), no date: Global seismic hazard map. globalquakemodel.org/product/ global-seismic-hazard-map (16 August 2025)

Graciano, L.E., Villaraza, C., Tamayo, C.P., Tamayo, M., Flordeliza, R., Quiaem, M.A., Ramos, J.M., 2020: Infrastructure damage analysis of the April 22, 2019 Pampanga, Philippines earthquake. *JSCE Journal of Disaster FactSheets*, FS2020-E-0002, 2020

Gavino, J.T., Ramos, E.E., Alberto, R.T., 2020: Site suitability mapping of onion in the province of Occidental Mindoro using Geographic Information System (GIS) model builder. *Philippine E-Journals, Science Asia Review* vol. 2, no. 1, ISSN 2719-0692, ejournals.ph/article.php?id=15837 (07 August 2025)

Hadlos, A., Opdyke, A., Ali Hadigheh, S.A., 2023: Deriving expert-driven seismic and wind fragility functions for non-engineered residential typologies in Batanes, Philippines. *Nature, Scientific Reports*, 13:22008 doig.org/10.1038/ s41598-023-49398-2

Housing and Land Use Regulatory Board (HLURB), 2013: A Guide to Comprehensive CLUP GUIDEBOOK Land Use Plan Preparation, vol. 1, p. 79. dhsud.gov.ph/wp-content/uploads/Publication/Guidebooks/HLURB_CLUP_Vol_1.pdf (14 August 2025)

Huang, H., Qiangzi Li, Q., Zhang, Y., 2019: Urban Residential Land Suitability Analysis Combining Remote Sensing and Social Sensing Data: A Case Study in Beijing, China. *Sustainability* 11, 2255; doi.org/10.3390/su11082255

Humanitarian Data Exchange (HDX), 2023: Philippines - Subnational Administrative Boundaries. data.humdata.org/dataset/cod-ab-phl (14 August 2025)

Joint Research Center of the European Commission, 2024 (last updated): River Flood Hazard Maps at European and Global Scale. data.jrc.ec.europa.eu/collection/id-0054 (15 August 2025)

Lin, H.L., 2015: Land Suitability Assessment for Disaster-prone Villages Relocation. *Int. J. of Safety and Security Eng*., Vol. 5, No. 1

Luan, C., Liu, R., Peng, S., 2021, Land-use suitability assessment for urban development using a GIS-based soft computing approach: A case study of Ili Valley, China. *Ecological Indicators*, Volume 123, doi.org/10.1016/j.ecolind.2020.107333

Malczewski, J., 2004: GIS-based land-use suitability analysis: a critical overview. *Progress in Planning*. 62 (1): 3–65.

Mas, E., Bricker, J., Kure, S., Adriano, B., Yi, C., Suppasri, A., Koshimura, S., 2014: Field survey report and satellite image interpretation of the 2013 Super Typhoon Haiyan in the Philippines. *Nat. Hazards Earth Syst. Sci. Discuss*., 2, 3741–3767, 2014. doi.org/10.5194/nhessd-2-3741-2014

Monteverde, M.A.C., Cinco, T.A., Hilario, F.D., Celebre, C.P., Tuddao, A., Ares, E., Arthur, W.C., 2014: Enhancing Risk Analysis Capacities for Flood, Tropical Cyclone Severe Wind and Earthquake for the Greater Metro Manila Area, ndrrmc.gov.ph/attachments/article/1509/Component_4_ Tropical_Cyclone_Severe_Wind_Technical_Report_-_Final_ Draft_by_GA_and_PAGASA.pdf (11 August 2025).

Morales, F., de Vries, W.T., 2021: Establishment of Land Use Suitability Mapping Criteria Using Analytic Hierarchy Process (AHP) with Practitioners and Beneficiaries. *Land*, 10(3), 235; doi.org/10.3390/land10030235

Murseli, R., Isufi, F., 2014: Land suitability location analysis for housing development using GIS. UBT International Conference. 18. knowledgecenter.ubt-uni.net/conference/ 2014/all-events/18 (13 August 2025)

National Aeronautics and Space Administration (NASA), no date: Cooperative Open Online Landslide Repository (COOLR). maps.nccs.nasa.gov/arcgis/apps/MapAndAppGallery/index.html?appid=574f26408683485799d02e857e5d9521 (12 August 2025)

National Hurricane Center, NHC, no date: Hurricanes and Tropical Cyclones. wx.erau.edu/faculty/mullerb/Wx365/ Hurricanes/hurricanes.html (20 August 2025)

National Oceanic and Atmospheric Administration (NOAA), no date: International Best Track Archive for Climate Stewardship (IBTrACS) data (accessed 07 July 2025)

Open Street Map (OSM), no date: Philippines. download.geofabrik.de/asia/philippines.html (16 August 2025)

Philippine Coconut Authority (PCA), 2023: Suitability maps and assessment protocols enhancement continues for a data-driven coconut industry. pcaarrd.dost.gov.ph/index.php /quick-information-dispatch-qid-articles/suitability-maps-and-assessment-protocols-enhancement-continues-for-a-data-driven-coconut-industry (15 August2025)

Philippine Statistics Authority (PSA), 2023: Housing Characteristics in the Philippines (2020 Census of Population and Housing), psa.gov.ph/content/housing-characteristics-philippines-2020-census-population-and-housing (12 August 2025)

Philippine Statistics Authority (PSA), 2025: A Total of 225 Small-Scale Natural Hazard Occurred in the Philippines in 2024 (with downloadable data in MS Excel format for 2015 to 2023), psa.gov.ph/content/total-225-small-scale-natural-hazard-occurred-philippines-2024?vcode=Rd60yt (06 August 2025)

Purwaamijaya, I.M., 2020, Land Suitability Evaluation for Housing and Residential Based on GIS, Satellite Imagery and DTM. doi.org/10.4108/eai.12-10-2019.2296328

Resilience Institute of the University of the Philippines (UPRI), no date: NOAH downloads. drive.google.com/drive/folders/ 1ALE4-E9c-4AGjm1fqiPprWHrLUskeY9o (12 August 2025)

Sadie, N.T., Tanchuling, M.A.N., Blanco, A.C., 2022: Landfill Site Suitability Mapping Using Fuzzy Multi-Criteria Decision Analysis and GIS: Case of Quezon City, Philippines. *PEJ*; Vol. 43, No. 1: 1-22

Sia, E.E.A., Navarra, N., Villa Juan, J.D., 2021: GIS-based land suitability analysis for potential urban development sites in Diffun, Quirino, Philippines. *IOP Conf. Series: Earth and Environmental Science* 879, 012002, doi.org/10.1088/1755-1315/879/1/012002

Suppasri, A., Mas, E., Charvet, I., Gunasekera, R., Imai, K., Fukutani, Y., Abe, Y., Imamura, F., 2013: Building damage characteristics based on surveyed data and fragility curves of the 2011 Great East Japan tsunami. *Nat Hazards*, 66:319–341, doi.org/10.1007/s11069-012-0487-8

Uhe, P., Hawker, L., Paulo, L., Sosa, J., Sampson, C., Neal, J., 2022: FABDEM - A 30m global map of elevation with forests and buildings removed. EGU General Assembly 2022, Vienna, Austria, 23–27 May 2022, EGU22-8994

United Nations Office for Disaster Risk Reduction (UNDRR), no date: Global model of cyclone wind 50, 100, 250, 500 and 1000 years return period. data.humdata.org/dataset/ cyclone-wind-100-years-return-period (20 August 2025).

University of the Philippines, School of Environmental Science and Management (SESAM), no date: Landslide Investigations on Geohazards for Timely Advisories in the Philippines (LIGTAS). upsystem.maps.arcgis.com/apps/webappviewer/index.html?id=43166f9436b5417a8c66692c2cadcf03 (22 August 2025)

Yang, T., Nadimpalli, K., Cechet, B. (Geoscience Australia), 2014: Local Wind Assessment in Australia, Computation Methodology for Wind Multipliers. Record 2014/33. Geoscience Australia, Canberra. doi.org/10.11636/Record.2014.033